

SURFACE AND SUBSURFACE STRUCTURAL MAPPING OF LOKOJA (SHEET 247), CENTRAL NIGERIA USING AIRBORNE MAGNETIC AND REMOTE SENSING DATA

Abstract

The main goal of this research is to evaluate the surface and subsurface structural framework of Lokoja and its surroundings using airborne magnetic and Shuttle Radar Topographic Mission (SRTM) data by applying image processing techniques that accentuate changes in magnetic intensity and topography. To explicate our aim, the residual magnetic intensity (RMI) data of the study was reduced to a magnetic pole (RTP) to centre the anomalies above their causative source after which, the data was subject to the first vertical derivative filter where the structures were delineated, this was done within Oasis Montaj software environment. Four (4) shaded relief images were created with light sources emanating from four different directions to identify linear terrain features in the SRTM data at a solar azimuth of 0° and a solar elevation of 45° . Others are 45° , 90° , and 135° followed by the creation of a composite shaded relief image that combined the four images produced. The PCI Geomatica edge detection algorithm was applied to the composite shaded relief image produced. After thresholding and filtering processes, structural lineaments were extracted from the edges of the image by subjecting it to the line algorithm of PCI Geomatica. ArcGIS v10.7.1 was used to assign geometry to both magnetic and SRTM structures delineated. The resulting structural lineaments were subjected to Rockworks where a rose diagram that depicts structural trends within the study area was produced. The lineaments delineated allow us to decipher that the area is dissected by numerous subsurface and surface linear structures and these lineaments trend predominantly in the NE-SE, WSW-ENE, NW-SE, and N-S directions. Overlying the lineaments drawn from the pair of data sets showed several sites of structural coincidence that are thought to be structural continuation locations where subsurface fluids such as water will probably migrate to the surface.

Keywords: Structural lineaments, aeromagnetic, RTP, SRTM, and Edge detection

Introduction

Geological structures (surface and subsurface) play a crucial role in groundwater exploration especially in the basement complex as water is hosted within the secondary structures (Faults, joints, and fractures), in dam design, the knowledge of the structural framework of a place provided by a geoscientist to the engineers can provide them with a clue on how the dam is to be designed (Tawey *et al.*, 2021; Netshithuthuni & Zvarivadza 2018). Also, these geologic structures are conduits that allow the flow of fluid into host rocks as such, they can host water, oil and ore minerals (Olivier *et al.*, 2011; Netshithuthuni & Zvarivadza 2018). In the delineation of these

geological structures that could aid in the establishment of a structural framework of the study area that is responsible for either water or mineral exploration, two sets of data have been used; these are the utilization of topographic data and airborne magnetic data. Hillshade maps produced from Shuttle Radar Topography Mission (SRTM), digital elevation model (DEM) has been used in several published research papers to delineate surface structures which are reflection of subsurface geologic structures (Maulana *et al.*, 2023; Rauf *et al.*, 2022; Manyoe & Hutagalung, 2022; Siombonea *et al.*, 2022; Tawey *et al.*, 2021; Agbebia & Eges, 2020; Fajri *et al.*, 2019; Manjare & Pophare, 2019; Akinluy *et al.*, 2018; Nugroho & Tjahjaningsih, 2016; Papadaki *et al.*, 2011).

Airborne magnetic surveys are a very important first step in geophysical exploration because they make it possible to find ambient magnetic fields produced by subsurface magnetic minerals (Gaafar, 2015), most of these magnetic minerals are associated with geologic structures as such, airborne magnetic data is the most widely used in the delineation of subsurface geologic structures for minerals (Telford *et al.*, 1990; Murphy, 2007). Integrating magnetic data and other methods has provided subsurface evidence of mineralisation or associated structures/alteration zones (Mohanty *et al.*, 2011; Chaturvedi *et al.*, 2013; Patra *et al.*, 2013; Gaafar, 2014, 2015). Works have been published employing airborne magnetic data for structures and mineralization (Tawey *et al.*, 2020a; Tawey *et al.*, 2021). Several other works have also been published employing the integration of airborne magnetic and remote sensing data for structural delineations (Ayuba & Nur, 2018; Faruwa *et al.*, 2021; Ogunmola *et al.*, 2015; Ebele & Nur, 2020; Tawey *et al.*, 2020b).

The goal of the present study is to carry out surface and subsurface structural mapping of Lokaja (sheet 247).

The objectives of the study are to Produce the first vertical derivative map of the area for subsurface structural delineation, produce a hillshades map of the study area for surface structural delineation carry out statistical structural analysis of the study area and produce a combined structural map showing areas of structural overlap between surface and subsurface structures.

The study area is bounded by longitude $6^{\circ}30'1''E$ to Longitude $7^{\circ}E$ and Latitude $7^{\circ}30'1''N$ to Latitude $8^{\circ}N$ and it is located within southcentral Nigeria, with the Nigeria confluence town (Lokoja), almost at the centre of it (Figure 1). Tectonically, it is situated within the Togo - Benin-Nigeria swell that is adjacent to the Togo belt, all of which are a product of the Pan African Orogeny and is bordered by the Volta Basin to the west, the Sokoto Basin that is the continuation of Iullemeden Basin in the north, the Chad Basin in the northeast and the Benue trough in the east (Figure 1). Geologically, the area is partly basement to the west and partly sedimentary to the east. The lithology within the study area is Banded gneiss/Biotite gneiss, Migmatite, Granite Gneiss, Undifferentiated older granite, River Alluvium, Undifferentiated Schist, False bedded sandstone, Coal, sandstone and shale, Mudstone and shale, Feldspathic sandstone and siltstone, Undifferentiated older granite, and Charnockitic Rocks (NGSA, 2006). Topographic variation within the study area varies from 0 m to 580 m above sea level (Figure 2). The Benue trough is a low land area with surface topography that varies from 60 m to 90 m below the surrounding areas, as revealed on the digital elevation map of the study area (Figure 2b).

Material and methods

Sources of Data Magnetic data

The Nigerian Geological Survey Agency (NGSA), Abuja, provided the airborne magnetic data that was utilised in this investigation. The Fugro airborne surveys used the following criteria to collect and process the data: 0.1 seconds or less (7m) for magnetic data recording interval, 80 meters for sensor mean terrain clearance, 500 meters for flight lines, 5000 meters for tie lines, 135 degrees for flight lines, and 45⁰ degrees for tie lines.

Sources of Remote sensing data

The Digital elevation model (DEM) by the Shuttle Radar Topographic Mission (SRTM) with serial number (n07_e006_1arc_v3.tif) was downloaded from the USGS website (<https://earthexplorer.usgs.gov/>) and has a spatial resolution of 30 m.

Methodology

The magnetic data was processed using Oasis Montaj software. This was done by first reducing the Residual magnetic intensity data to the pole (RTP) using inclination and declination angle values of (-9.45⁰ and -2.15⁰) with Amplitude inclination correction of -90⁰. The first vertical derivative filter was then applied to the RTP for magnetic structural delineation. Also, the RTP data was subjected to Euler deconvolution with a structural index equal to 1 for structural delineation. Hillshade maps using four distinct solar azimuths of 0°, 45°, 90°, and 135° followed by the creation of a composite shaded relief image that combined the four images produced (Figure 3). The PCI Geomatica's edge detection algorithm was applied to the composite shaded relief image produced. After thresholding and filtering processes, structural lineaments were extracted from the edges of the image by subjecting it to the line algorithm of PCI Geomatica. ArcGIS v10.8 was used to assign geometry to both magnetic and SRTM structures. The resulting

structural lineaments were subjected to Rockworks where a rose diagram that depicts structural trends within the study area was produced for both surface and subsurface structures.

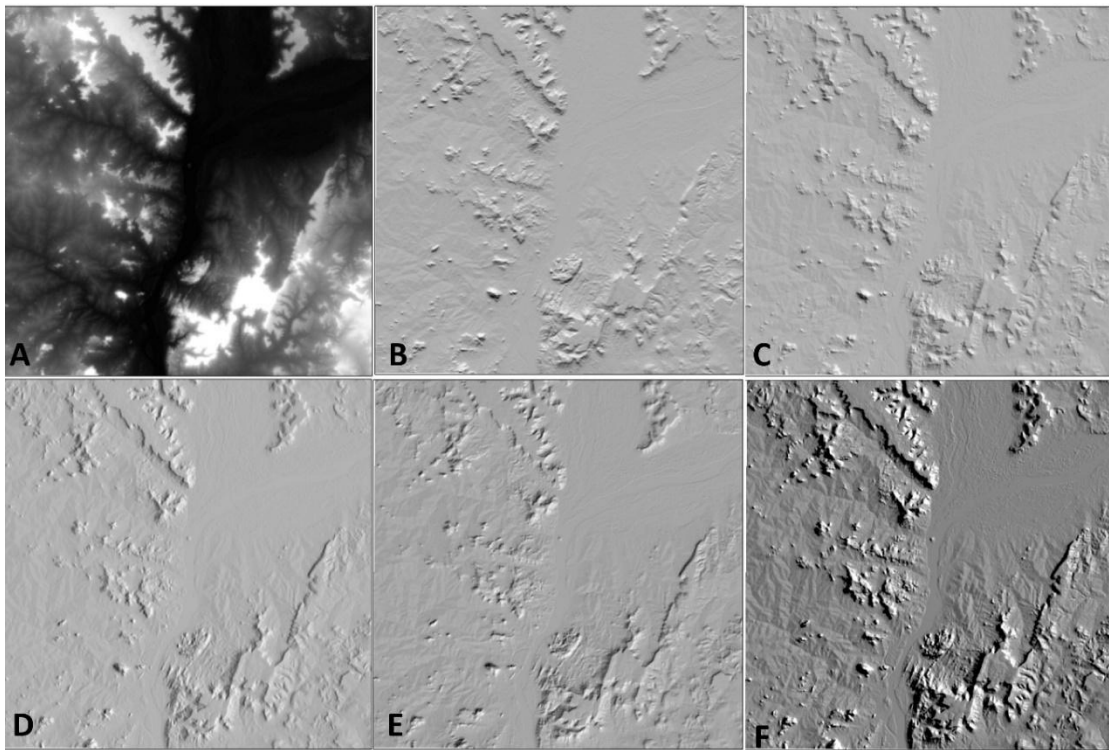


Figure 3: a. SRTM DEM of the study area with a solar azimuth of b. 0°, c. 45°, d. 90° and 135° hillshade maps and F. the combined hillshade map

Theory of the methods

Vertical derivatives

Vertical derivative filters are typically applied to magnetic grids using fast Fourier transform (FFT) filters. They enhance short-wavelength components of the magnetic field (Foss, 2011), and can be achieved by multiplying the field's amplitude spectra by a factor.

$$\frac{1}{n} \left[(U^2 + V^2)^{\frac{1}{2}} \right]^n \quad 1$$

where n is the order of the vertical derivative, and (U, V) is the wavenumber corresponding to the (x, y) directions respectively.

Results and Discussion

The residual magnetic intensity map of the study area is represented by Figure 4a while the residual magnetic intensity reduced to the pole map of the study area is represented by Figure 4b. From Figure 4a, the susceptibility value varies from -113.753 nT low to 134.876 nT high. High susceptibility values are observed around Okuma, Mozum, Okpai, an area south of Lokoja and Zongodaji to the western end of the map. Magnetic lows are observed around the north of Kuroko, Adama, Oko and Yanemi. Furrow-like feature trending Northeast to southwest is a prominent structure cutting across the study area from the western end of the map around latitude $7^{\circ}55' W$ to northeast. Magnetic low within this furrow-like feature is attributed to weathering and metasomatic activities with the structure leading to the depreciation of magnetite within these areas resulting in low magnetic susceptibility. From the west to the centre of the map is a dyke a feature that is trending east-west but as the structure approaches the centre of the map, the trend changes to NE-SW.

The alternating occurrence of magnetic low and high around the south and west of Ajaokuta is also attributed to the presence of structures within this area. While Figure 4b displays the reverse in

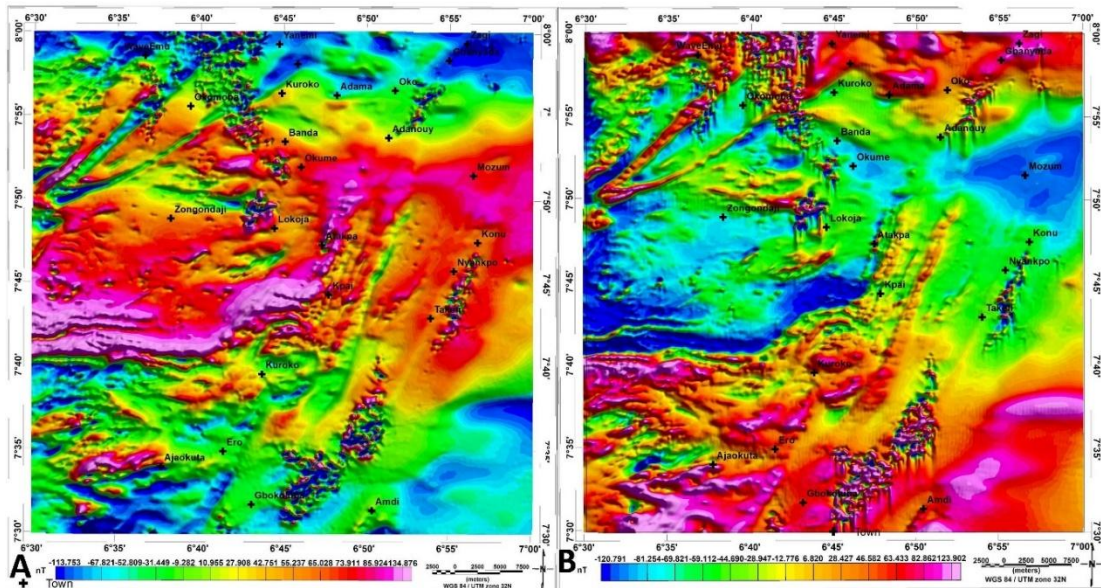


Figure 4: a. Residual magnetic intensity and b. Residual magnetic intensity reduced to the pole

magnetic susceptibility of the study area. Anomalies are directly placed on the causative sources. Low areas such as the north of Kuroko, Adama, Oko and Yanemi in Figure 4a are now showing magnetic high while areas showing magnetic high in Figure 4a such as Okuma, Mozum, Okpai, the area around south of Lokoja and Zongodaji to the western end of the map are now showing magnetic low intensity. Also, susceptibility within this map varies from -120.791nT low to 123.902 nT high. Generally, the middle of this map from west to east shows low magnetic susceptibility while the north and southern portions both from east to west are showing magnetic highs.

Figure 5a represents the first vertical derivative map of the study area highlighting the structures within this area. while Figure 5b represents the first vertical derivative map with delineated subsurface structures overlaid on it in the black strike. From Figures 5a and 5b, sedimentary portions can be distinguished from the basement portion of the map based on the structural occurrences within the basement part of the study area. Structures are seen to occur majorly within the basement part of the study area in the west and southwestern part of the study area.

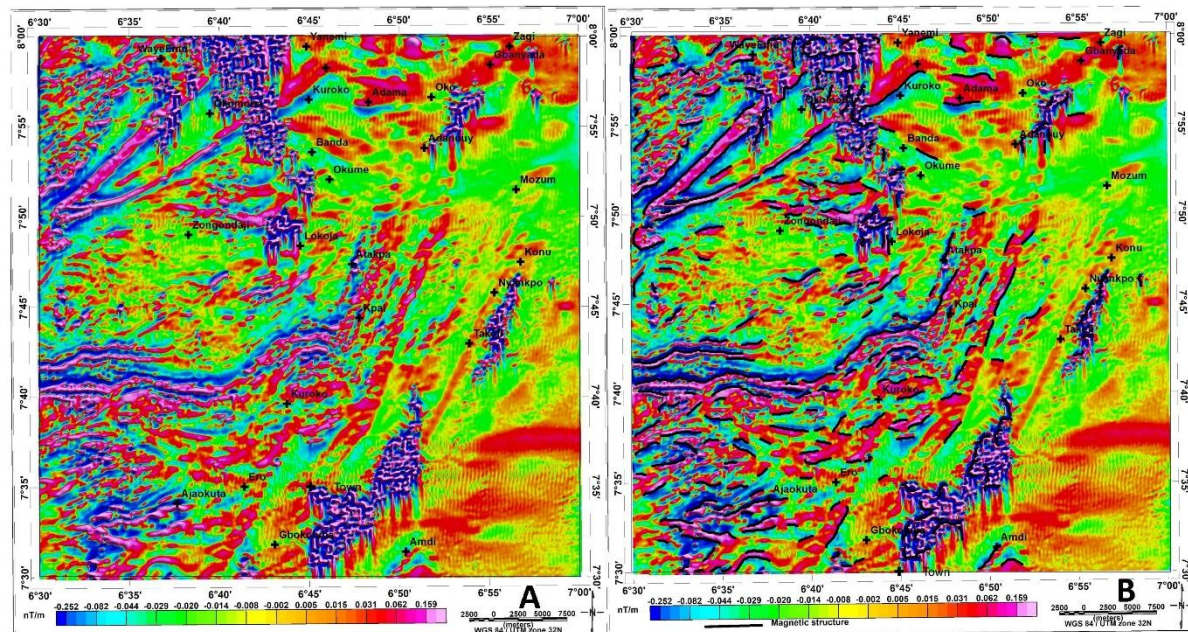


Figure 5: a. first vertical Derivative map and b. First vertical derivative map with structures

The occurrence of short wavelengths around the northeastern portion of the map and north central portion is attributed to shallow sedimentary thickness or shallow depth to magnetic source.

Subsurface Structural Trend

The subsurface structures overlaid on the grayscale map of the first vertical derivative also showing the confluence of river Niger and Benue is represented by Figure 6 while Figure 6b represents the subsurface structural density map of the study area. the statistical trend map of the study area is represented by the Rose diagram (Figure 6c). From Figure 6a, structures are observed to occur primarily in the basement portion and the sedimentary portions that are relatively thin (shallow depth to the magnetic source), especially the eastern part of the study area from north to south. The subsurface structural density is high within the western part of the study area.

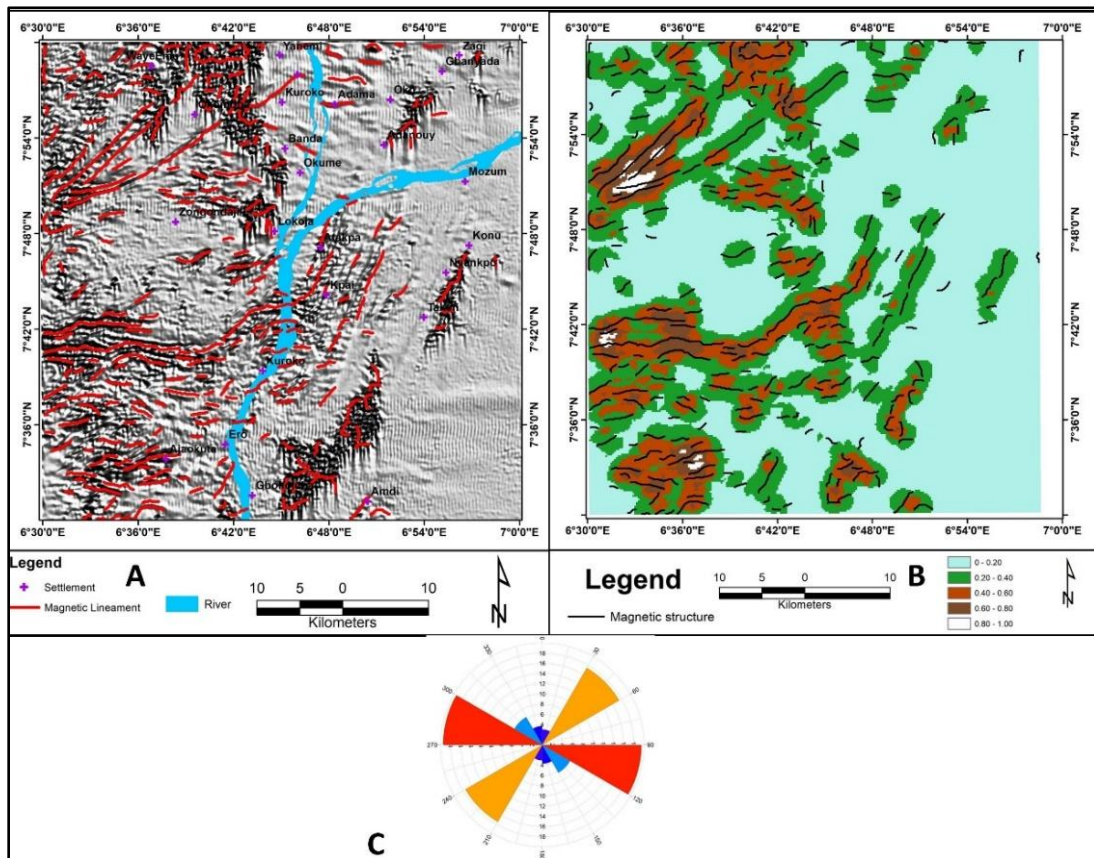


Figure 6: a. Grayscale first vertical Derivative map with subsurface structures, b. subsurface structural density (km/km^2) map and c. Rose diagram

Tectonic activities that affected the basement complex of Nigeria left its imprints which are structures or lineaments (fracture, fault, and joints) with a particular trend. In this study trend analysis carried out has revealed five tectonic trends. The most predominant of them is the West-north-west to East-south-east (WNW-ESE) followed by the Northeast to southwest (NE-SW), North-west to South-east (NW-SE)

Surface Structural Trend Analysis

Figure 7a represents the hillshade map of the study area while 7b represents the delineated topography or surface structures overlaid on the hillshade map. From Figure 7b surface structures are observed to occur predominantly within the southwest, northwest, and northeastern

portion of the map. The surface structures are not predominant in the basement like the sedimentary portion of the area. Within the southcentral portion of the area to the south, rocks with surface structural occurrences are undifferentiated Schist including Phyllites, banded Gneiss, Coal, sandstone, and shale. Within the feldspathic sandstone and siltstone in the north, topographic structures are seen to be concentrated here. Figure 9a reveals the structural density of the surface structures, and the southeast and northwest portions of the study area have the highest surface structural density 0.8 to 1.0 km/km². Surface structural trends have been statistically analysed using a rose diagram (Figure 8b) that reveals the most predominant surface structural trend to NNE-SSW, followed by NNW to SSE, NW-SE, NE-SW, WNW-ESE and lastly, the ENE-WSW trend. The integration of the subsurface and surface structures has revealed points or areas of structural continuation where fluid from the subsurface find its way to the surface. These points of structural overlap have been demarcated using a purple polygon (Figure 10).

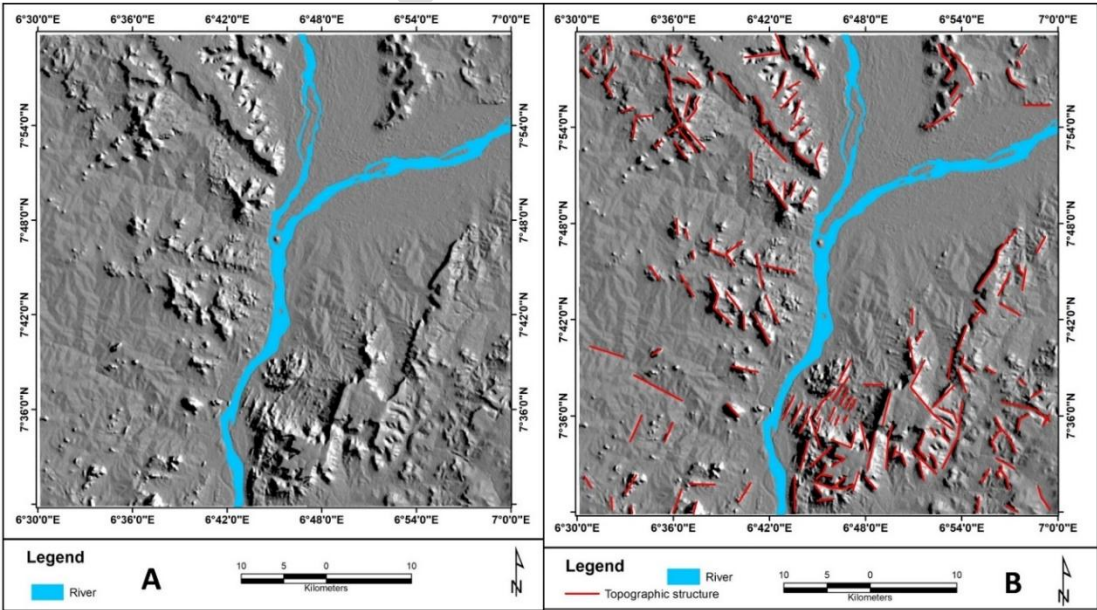


Figure 7: a. Combined hillshade map and b. Hillshade map with surface structures

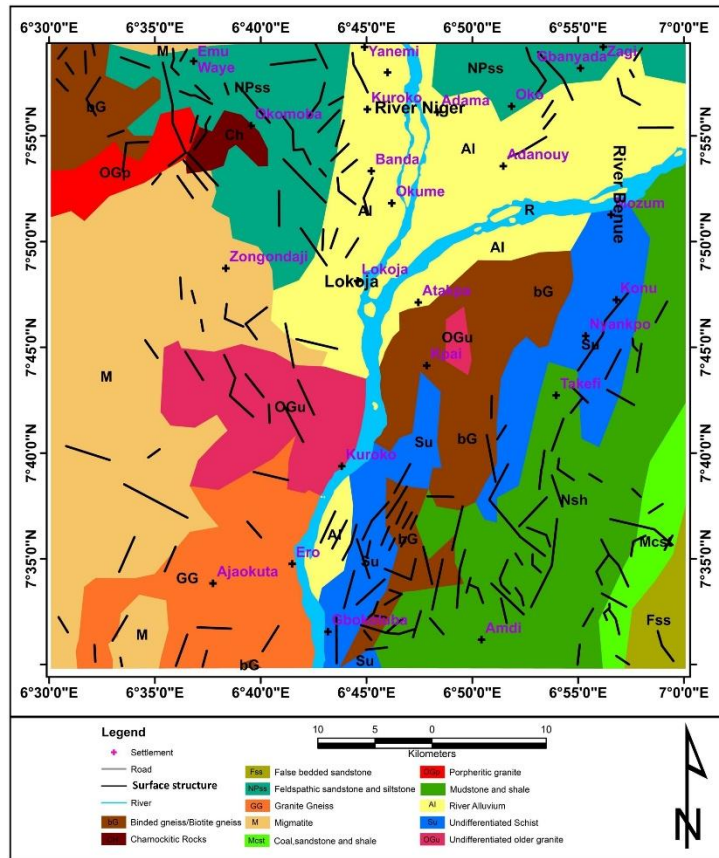


Figure 8: Geologic map of the study area with topography structures

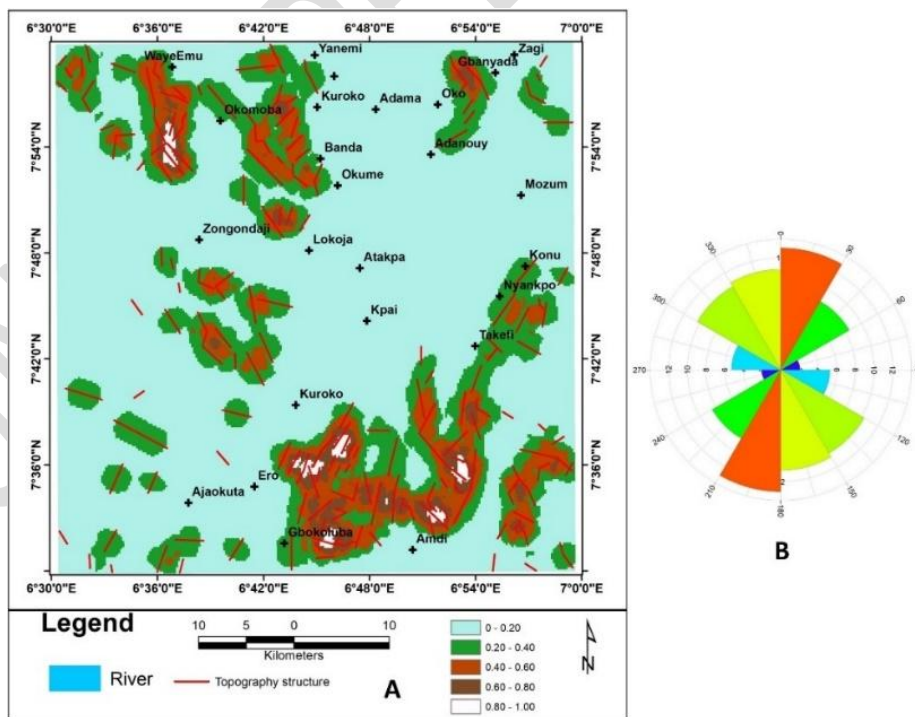


Figure 9: a. Surface structural density map and b. Rose diagram

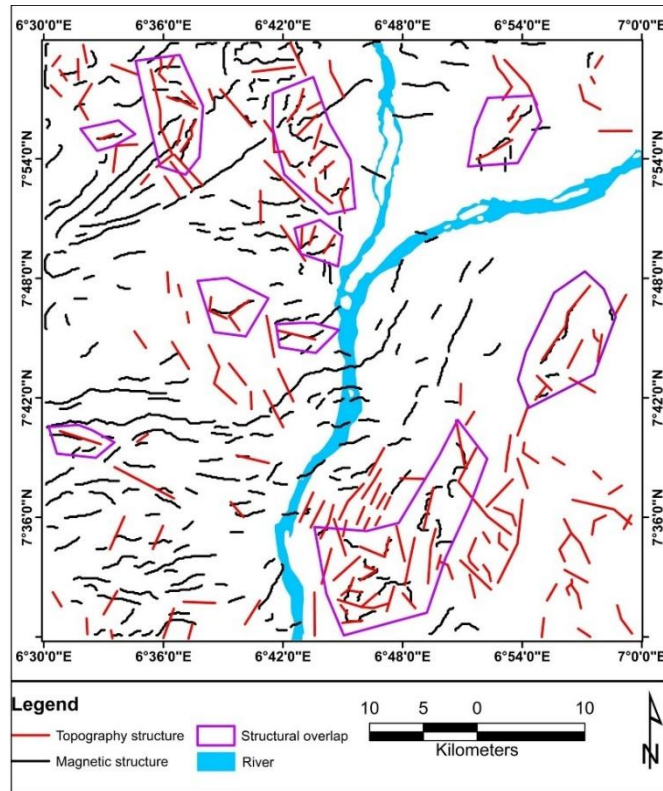


Figure 10: Combine surface (Topographic) structures and subsurface (Magnetic) structures showing areas of structural overlap

Conclusion

The study area exhibits subsurface magnetic structures primarily in the basement and sedimentary portions with thin sedimentary cover, especially in the eastern part of the area, and the subsurface structural density is high in the west of the area. There are four major tectonic trends revealed based on the analysis of the airborne magnetic data of the study area: West-northwest to east-southeast (WNW-ESE), Northeast to southwest (NE-SW), and Northwest to south-east (NW-SE).

The southwest, northwest, and northeastern regions of the research area are predominately made up of topographic (surface) structures. The largest surface structure density is found in the southeast and northwest. The investigation of surface structural trends has shown that the NNE-SSW surface structural trend is the most prevalent, followed by NNW to SSE, NW-SE, NE-SW,

WNW-ESE, and ENE-WSW. Within the study area, there are regions of structural overlap that have been identified using purple polygons.

References

Agbebia and Eges (2020) Lineament Analysis and Inference of Geological Structures in Bansara-Boki Area, Southeastern Nigeria *Asian Journal of Environment & Ecology*, AJEE, 13(1): 28-44

Akinluyi, F. O., Olorunfemi, M. O., & Bayowa, O. G (2018) Investigation of the influence of lineaments, lineament intersections and geology on groundwater yield in the basement complex terrain of Ondo State, Southwestern Nigeria. *Applied Water Science*. 8:49

Ayuba, R., & Nur, A. (2018). Analysis of High-Resolution Aeromagnetic Data and Satellite Imagery for Mineral Potential Over Parts of Nasarawa and Environs, North-Central Nigeria. *International Journal of Scientific & Technology Research*, 7(6), 103.

Chaturvedi, A.K., Lotter, C., Tripathi, S., Maurya, A.K., Patra, I., Parihar, P. S., (2013). Integrated application of heliborne and ground electromagnetic surveys for mapping EM conductor for uranium exploration and its subsurface validation, North Delhi Fold Belt, Rajasthan, India: a case study. *Geophysics* 78 (1), B13–B24.

Ebele, J. E., & Nur, A. (2020). Regional groundwater studies using high-resolution aeromagnetic data in Abuja and environs, North-Central Nigeria. *Applied Journal of Physical Science*, 2(3), 68-79.

Fajri, S. N., Surtiyono, E., & Nalendra, S. (2019) Lineament analysis of digital elevation model to identification of geological structure in Northern Manna Sub-Basin, Bengkulu. IOP Conference. Series: Materials Science and Engineering 636, 012001

Faruwa, A. R., Qian, W., Akinsunmade, A., Akingboye, A. S., & Dusabemariya, C. (2021). Aeromagnetic and remote sensing characterization of structural elements influencing iron ore deposits and other mineralization in Kabba, southwestern Nigeria.

Foss, C. (2011). Magnetic data Enhancement and Depth Estimation. In H. Gupta (Ed.), *Encyclopedia of Earth Sciences Series*, 736-746.

Gaafar, I. M. (2012). Geophysical signature of the vein-type uranium mineralisation of Wadi Eishimbai, Southern Eastern Desert, Egypt. *Arabian Journal of Geoscience*, 5, 1185–1197.

Gaafar, I. M. (2014). Geophysical mapping, geochemical evidence and mineralogy for Nuweibi rare metal albite granite, Eastern Desert, Egyptian. *Open Journal of Geology*. 4, 108–136.

Gaafar, I. (2015). Integration of geophysical and geological data for delimitation of mineralized zones in Um Naggat area, Central Eastern Desert, Egypt. *NRIAG Journal of Astronomy and Geophysics*, 4, 86–99.

Manjare, B.S., & Pophare, A. M. (2019) Lineament Mapping Using Shaded Relief Images Derived from Digital Elevation Model. *Journal of Geosciences Research*. 4(2); 155-161

Manyoe, I. N., & Hutagalung, R (2022) Application of Lineament Density Extraction Based on Digital Elevation Model for Geological Structures Control Analysis in Suwawa Geothermal Area *Journal of Geoscience, Engineering, Environment, and Technology* 7(3), 117-133

Maulana, B. R., Burhanuddin, M. S., & Akbar, M. F. (2023). Lineament Density and Implications for the Distribution of Ground Fissures After 2021 MW 7.3 Flores Sea Earthquake on Kalaotoa Island, Indonesia. *Journal of Geoscience, Engineering, Environment, and Technology*; 8 (1)

Mohanty, W. K., Mandal, A., Sharma, S. P., Gupta, S., Misra, S. (2011). Integrated geological and geophysical studies for delineation of chromite deposits: a case study from Tangarparha, Orissa, India. *Geophysics* 76, B173–B185.

Murphy, B. S. (2007). Airborne geophysics and the Indian scenario. *Journal of Indian Geophysical Union* 11 (1), 1–28.

Netshithuthuni, R., Sengani, F., & Zvarivadza, T. (2018). Application of Aeromagnetic, Remote Sensing and Geological Data in the Delineation of the Geological Structures. *International journal of georesources and environment*, 4(3), 141-146.

NGSA. (2006). *Geology and Structural Lineament Map of Nigeria*.

Nugroho, U. C & Tjahjaningsih, A (2016). Lineament density information extraction using dem srtm data to predict the mineral potential zones. *International Journal of Remote Sensing and Earth Sciences* 13(1), 67-74

Obaje, N. G. (2009). *Geology and Mineral Resources of Nigeria*. Berlin: Springer-Verlag, Heidelberg.

Ogunmola, J.K., Gajere, E.N. Ayolabi., E. A. Olobaniyi, S.B., Jeb, D.N., & Agene, I.J. (2015) Structural study of Wamba and Environs, north-central Nigeria using aeromagnetic data and Nigeria Sat-X image. *Journal of African Earth Sciences*, Vol 111, Pp 307-321. <https://doi.org/10.1016/j.jafrearsci.2015.07.028>

Olivier, J., Vente, J.S. & Jonker, C.Z. (2011). Thermal and chemical characteristics of hot water springs in the northern part of the Limpopo Province, South Africa. *Water SA*, 37(4), 427 - 436.

Sabins, F. F. (1997). *Remote Sensing: Principles and Interpretation*. W.H. Freeman and Company, New York, p. 361.

Papadaki, E. S., Mertikas, S. P., & Sarris, A. (2011). Identification of lineaments with possible structural origin using ASTER images and DEM-derived products in Western crete, Greece. *EARSel eProceedings*, 9-26

Patra, I., Chaturvedi, A. K., Srivastava, P. K., & Ramayya, M. S. (2013). Integrated interpretation of satellite imagery, aeromagnetic, aeroradiometric and ground exploration data sets to delineate favourable target zones for unconformity-related uranium mineralisation, Khariar Basin, Central India. *Journal Geological Society India* 81, 299–308.

Rauf, j., Kayambo, M. R., Nurjana, I., & Manyoe, I. N. (2022) Lineament Extraction Analysis Using Digital Elevation Model (DEM) in Lahendong Geothermal Area, North Sulawesi. *E3S Web of Conferences* 400, 01009

Siombonea, S.H., Susilob, D., & Maryantob., S (2022) Integration of Topex Satellite Gravity and Digital Elevation Model Shuttle Radar Topography Mission (DEM SRTM) Imagery for Subsurface Structure Identification at Tiris Geothermal Area. *Positron* 12 (2), 98-111

Tawey, M. D., Alhassan, D. U., Adetona, A. A., Salako, K. A., Rafiu, A. A., & Udesi, E. E. (2020a). Application of Aeromagnetic Data to Assess the Structures and Solid Mineral Potentials in Part of North Central Nigeria. *Journal of Geography, Environment and Earth Science International*, 24(5), 11-29. DOI: 10.9734/JGEESI/2020/v24i530223.

Tawey, M. D., Alhassan, D. U., Adetona, A. A., Salako, K. A., Rafiu, A. A., & Udesi, E. E. (2020b). Edge Detection and Depth to Magnetic Source. Estimation in Part of Central Nigeria. *Physical Science International Journal*, 24(7), 54-67. DOI: 10.9734/JGEESI/2020/v24i530223.

Tawey, M. D., Adetona, A.A., Alhassan, U. D., Rafiu, A. A., Kazeem A. Salako, K. A & Udensi E. E (2021). Aeroradiometric Data Assessment of Hydrothermal Alteration Zones in Parts of North Central Nigeria. *Asian Journal of Geological Research*. 4(2): 1-16, 2021; Article no. AJOGER.67062

Tawey M. D., Adesoji, I. A., & Jiriko A. H., (2021) Surface and Subsurface Lineament Studies of Gitata (Sheet 187) Using Aeromagnetic and Remote Sensing Data 10th National Water Conference Benin, Edo State, Nigeria

Telford, W. M., Geldart, L. P., & Sheriff, R. E. (1990). *Applied Geophysics*. Cambridge University Press, second edition

Wright, J. B. (1985). *Geology and Mineral Resources of West Africa*.

UNDER PEER REVIEW